Neuropsychopharmacology (2014) 39, 2662–2672

www.neuropsychopharmacology.org

Cellular and Behavioral Outcomes of Dorsal Striatonigral Neuron Ablation: New Insights into Striatal Functions

Delphine Révy[1,5], Florence Jaouen[1,5], Pascal Salin[1], Christophe Melon[1], Dorian Chabbert[1], Elisiana Tafi[2], Lena Concetta[2], Francina Langa[3], Marianne Amalric[4], Lydia Kerkerian-Le Goff[1], Hélène Marie[2,6] and Corinne Beurrier*[,1]

[1]Institut de Biologie du Développement de Marseille (IBDM), Aix-Marseille University (AMU), Centre National de la Recherche Scientifique (CNRS), UMR 7288, Marseille Cedex 9, France; [2]The European Brain Research Institute, Roma, Italy; [3]Institut Pasteur, Mouse Genetics Engineering Center, Paris Cedex 15, France; [4]Laboratoire de Neurosciences Cognitives, Aix-Marseille University, Centre National de la Recherche Scientifique (CNRS), UMR 7291, Marseille Cedex 3, France

The striatum is the input structure of the basal ganglia network that contains heterogeneous neuronal populations, including two populations of projecting neurons called the medium spiny neurons (MSNs), and different types of interneurons. We developed a transgenic mouse model enabling inducible ablation of the striatonigral MSNs constituting the direct pathway by expressing the human diphtheria toxin (DT) receptor under the control of the Slc35d3 gene promoter, a gene enriched in striatonigral MSNs. DT injection into the striatum triggered selective elimination of the majority of striatonigral MSNs. DT-mediated ablation of striatonigral MSNs caused selective loss of cholinergic interneurons in the dorsal striatum but not in the ventral striatum (nucleus accumbens), suggesting a region-specific critical role of the direct pathway in striatal cholinergic neuron homeostasis. Mice with DT injection into the dorsal striatum showed altered basal and cocaine-induced locomotion and dramatic reduction of L-DOPA-induced dyskinesia in the parkinsonian condition. In addition, these mice exhibited reduced anxiety, revealing a role of the dorsal striatum in the modulation of behaviors involving an emotional component, behaviors generally associated with limbic structures. Altogether, these results highlight the implication of the direct striatonigral pathway in the regulation of heterogeneous functions from cell survival to regulation of motor and emotion-associated behaviors.
Neuropsychopharmacology (2014) **39,** 2662–2672; doi:10.1038/npp.2014.121; published online 9 July 2014

INTRODUCTION

The basal ganglia (BG) are key neural substrates that control motor and reward-associated behaviors. Their dysfunction is associated with several disorders, including Parkinson's disease (PD), schizophrenia, and drug addiction (Cenci, 2007; Graybiel, 2000; Lobo and Nestler, 2011). As the main BG input, the striatum is thought to be an important site for mediating many of the maladaptive processes responsible for these devastating neurological disorders.

The striatum is classically delineated into dorsal (dorsal striatum) and ventral (nucleus accumbens) territories, involved in cognitive/motor and emotional/motivational functions, respectively. However, interconnections and other crosstalk, in particular involving the dopamine systems, provide an anatomical basis for a multifunctional interface (Haber *et al*, 2000). The dorsal striatum receives heavy dopaminergic input from the substantia nigra pars compacta (SNc), and dysfunction of dopamine signaling is implicated in almost all BG-associated disorders. The major striatal targets of dopamine afferents are the GABAergic medium spiny neurons (MSNs) which constitute 95% of the striatal population. The remaining neurons, comprising approximately 5% of the total number of striatal neurons, are made up of different subtypes of GABAergic interneurons and of cholinergic interneurons. Despite being few in number, cholinergic interneurons are crucial for the tuning of striatal output owing to their dense terminal fields primarily directed to the two populations of MSNs that overlap those of dopaminergic neurons (Bolam *et al*, 1984). The two types of MSNs are distinguished depending on their projections and expression of distinct set of proteins. MSNs that project primarily to the substantia nigra pars reticulata (SNr), so-called direct-pathway or striatonigral MSNs, express the dopamine D_1 receptor, substance P (SP) and dynorphin, whereas MSNs that project to the globus

*Correspondence: Dr C Beurrier, Institut de Biologie du Développement de Marseille (IBDM), Aix-Marseille University (AMU), Centre National de la Recherche Scientifique (CNRS), UMR 7288, Parc Scientifique de Luminy, Case 907, Marseille 13288, France, Tel: +33 491 26 92 48, Fax: +33 491 26 92 44,
E-mail: corinne.beurrier@univ-amu.fr
[5]These authors contributed equally to this work.
[6]Current address: Institut de Pharmacologie Moléculaire et Cellulaire (IPMC), Université de Nice Sophia Antipolis, Centre National de la Recherche Scientifique (CNRS), UMR 7275, Valbonne 06560, France.
Received 2 December 2013; revised 18 April 2014; accepted 16 May 2014; accepted article preview online 6 June 2014

pallidus (GP), so-called indirect or striatopallidal MSNs, express the dopamine D_2 receptor and enkephalin (Enk) (Gerfen *et al*, 1990; Smith *et al*, 1998). Because of the differential expression of dopamine receptors, the striatonigral and striatopallidal MSNs are thought to have opposing but balancing roles on BG output and behaviors (Albin *et al*, 1989; DeLong, 1990).

Recent advances in cell-type-specific technologies have provided a wealth of data allowing a more comprehensive understanding of MSNs roles in drug addiction (Durieux *et al*, 2009; Durieux *et al*, 2012; Ferguson *et al*, 2011; Lobo *et al*, 2010), cognitive functions (Hikida *et al*, 2010; Hikida *et al*, 2013; Nishizawa *et al*, 2012; Tai *et al*, 2012; Yawata *et al*, 2012), and parkinsonian physiopathology (Kravitz *et al*, 2010). Here, we developed a new inducible model of diphtheria toxin (DT) receptor-mediated ablation to further explore the functional implications of striatonigral MSNs of the dorsal striatum. For behavioral characterization, we first focused on motor function linked to disturbed striatal dopamine tone, cocaine-induced locomotion, and L-DOPA-induced dyskinesia (LID), which are associated with selective and robust molecular changes in striatonigral MSNs, including ERK signaling (Bertran-Gonzalez *et al*, 2008; Santini *et al*, 2009). Acute response to psychostimulant has been investigated using amphetamine in a model of striatonigral MSNs ablation restricted to subterritories of the dorsal striatum (Durieux *et al*, 2012), and direct demonstration of dorsal striatonigral MSNs involvement in LID, a major complication of the most common pharmacotherapy of PD, is still lacking. We next moved to non-motor function as accumulating evidence suggests that, in addition to sensorimotor information processing, the dorsal striatum might also mediate emotional/motivational functions classically ascribed to the ventral striatum (Balleine *et al*, 2007). We focused on anxiety behavior, notably because SP and dynorphin, two molecules released by striatonigral MSNs, have been implicated in the regulation of anxiety (Ebner and Singewald, 2006; Van't Veer and Carlezon, 2013).

The results show that ablation of striatonigral MSNs impacts heterogeneous functions from motor- and emotional-associated behaviors to region-specific regulation of cholinergic homeostasis.

MATERIALS AND METHODS

Generation of Transgenic Mice

The human Diphtheria Toxin Receptor-green fluorescent protein (DTR-GFP) cDNA was inserted in front of the endogenous ATG in exon 1 of the *Slc35d3* gene in a 196-kilobase mouse bacterial artificial chromosome (BAC) (RP23-344M6) by homologous recombination using the recombineering plasmid pL451. DNA from the modified BAC was purified and microinjected into pronuclei of fertilized mouse eggs (B65JL/F1) to generate transgenic founders (Mouse Genetics Engineering Center, Institut Pasteur). A total of five transgene-positive founders were obtained and were bred with C57Bl/6 mice. Offspring consisted of an equal number of DTR-expressing mice (DTR^+) and of DTR non-expressing mice (DTR^-).

Stereotaxic Injections

All animal experimental procedures were carried out in strict accordance with local rules concerning the use of laboratory animals (authorization no.B 13-464) and with the recommendations of the EEC (2010/63/UE) for care and use of laboratory animals and conformed to the ethical guidelines of the French Ministry of Agriculture and Forests (Animal Health and Protection Veterinary Service).

Surgery was performed on 8–12 week-old mice under xylazine/ketamine anesthesia (intraperitoneal injections, 10 and 100 mg/kg, respectively). All stereotaxic coordinates are listed in Supplementary Table S1. DT, (Calbiochem, Darmstadt, Germany) was diluted to a concentration of 0.5 ng/μl, and 1 μl was injected at two sites either into the dorsal striatum or into the nucleus accumbens. For retrograde tracing, 1 μl of fluorescent microbeads (Life Technologies, Saint-Aubin, France) were injected into the SNr. For dopaminergic lesion, mice received one unilateral injection (1.5 μl) of 6-hydroxydopamine hydrochloride (6-OHDA; 2.7 μg/μl; diluted in 0.9% sterile NaCl containing 0.1% ascorbic acid; Sigma-Aldrich, St Quentin-Fallavier, France) into the SNc.

Quantitative *In Situ* Hybridization and Dopamine Transporter Autoradiography

Radioactive *in situ* hybridization histochemistry was performed as described previously (Salin *et al*, 2002). Probes were 44–56 mer synthetic oligonucleotides selected on the basis of the sequence of *Tac1* (which encodes SP; hereafter called *SP*), *Penk* (which encodes Enk; hereafter called *Enk*), *GAD 67*, and tyrosine hydroxylase (*TH*) and were 3′-end-labeled by terminal deoxynucleotide transferase with ^{35}S-dATP. ^{3}H-mazindol was used as a ligand to label dopamine transporter sites. Briefly, after appropriate washes, sections were incubated with 15 nM [^{3}H]-mazindol (DuPont NEN Research Products, Boston, MA; specific activity, 17 Ci/mmol) in a Tris buffer containing 0.3 mM desipramine to block the noradrenalin uptake sites.

Quantitative RT-PCR

The uninjected and injected dorsal striatum of three DTR^+ mice injected with DT into the dorsal striatum were punched separately. Specific primers for the different genes of interest were designed using the Universal ProbeLibrary (ProbeFinder version 2.5 for mouse, Roche Diagnostics) and chosen intron-spanning when possible (Supplementary Table S2). Total RNA (170 ng) was reverse transcribed for 5 min at 25 °C, 30 min at 42 °C and 5 min at 85 °C using iScript Reverse Transcription Supermix for RT-qPCR (BIO-RAD). A Bio-Rad CFX96 cycler was used with the following cycling parameters: 1 cycle at 95 °C for 8 min, 40 cycles at 95 °C for 15 s followed by 60 °C for 1 min. Samples were run in three replicates for each gene. Relative target gene concentration was calculated using the $2^{-\Delta\Delta Ct}$ method (Livak and Schmittgen, 2001), which uses normalization to β-actin endogenous reference gene (as described in Lobo *et al*, 2006) and normalization to calibrator sample (here, uninjected dorsal striatum side).

Dual Fluorescence *In Situ* Hybridization

Two-color fluorescent *in situ* hybridization was performed with a mixture of fluorescein-labeled antisense riboprobe for ChAT or SP and a digoxigenin-labeled riboprobe for DTR. After appropriate pretreatments, sections were incubated at 65 °C overnight in the hybridization mix containing 400 ng/ml of both probes. After posthybridization washes, sections were incubated for 5 h with anti-Fluorescein-POD (HRP) (1/300) (Roche-Applied Science), and the fluorescein probe was visualized in green with fluorescein-tyramide reagent (TSA Plus PerkinElmer Life Sciences). After inactivating the HRP conjugate of the anti-Fluorescein-POD antibody (3% H_2O_2), the digoxigenin probe was then visualized in red with anti-digoxigenin-POD antibody (1/300) followed by cyanine-3-tyramide reagent.

Immunohistochemistry

Mice were perfused transcardially with ice-cold 4% paraformaldehyde in 0.1 M phosphate-buffered saline (PBS, pH 7.4). After overnight postfixation, brains were protected in a PBS solution containing 30% sucrose and frozen. Cryostat sections (40 μm) were incubated overnight at 4 °C with primary antibodies and then incubated with the appropriate secondary antibodies (Supplementary Table S3).

Data Analysis

Analysis of DT-mediated effects in the striatum was performed on 4–6 coronal sections per animal extending from AP = +1.54 to 0.14 relative to bregma according to the mouse stereotaxic brain atlas of Paxinos and Franklin (Second edition, 2001).

Single-Cell RT-PCR

Coronal striatal slices (250 μm) from DTR^+ mice were prepared and recorded as previously described (Beurrier *et al*, 2009). After cell-attached and whole-cell recordings, the cell content was aspirated, expelled into a test tube where the RT reaction was performed overnight at 40 °C. The single-cell RT-PCR protocol used here was adapted from Lena *et al* (1999) to simultaneously detect the expression of *DTR-GFP* and *ChAT* mRNAs. Genomic DNA amplification was systematically assessed using a NMDA receptor gene intron (NR1 subunit, *GRIN1*) as genomic control (Supplementary Table S4). The cDNAs were first amplified by 20 PCR cycles (94 °C, 1 min; 60 °C, 1 min; 72 °C, 1 min) using 5 U of *Taq* polymerase (Qiagen, Hilden, Germany), and 10 pmol of different sets of primers (Supplementary Table S3) were added (final volume, 100 μl). Second rounds of PCR (40 cycles as described above) were then performed using 6 μl of the first PCR product as a template (final volume 50 μl). Each cDNA was amplified individually using its specific primer generating PCR fragments of 406, 323 and 162 bp for *DTR-GFP*, *ChAT* and *GRIN1* introns, respectively.

Behavioral Tests

Mice were group-housed (2–5 mice/cage) and maintained on a 12 : 12-h light–dark cycle (0700 hours lights on) with *ad libitum* food and water available.

Locomotor activity. Locomotor activity was monitored in individual activity chambers (11.2 cm × 20.7 cm) housed within a sound-attenuating cubicle and under homogenous light illumination (Imetronic, Pessac, France). Each chamber was equipped with four infrared photobeams located 1.5 cm above floor level, two at the rear and two at the front of the chamber. Mice were given i.p. injections of saline (0.9% NaCl) for the first 3 testing days to habituate them to the injections, handling, and activity chambers. On the fourth day, mice of each genotype were divided into two groups receiving either i.p. injections of saline (0.9% NaCl) or cocaine hydrochloride (5 or 15 mg/kg; Sigma-Aldrich). Locomotor activity was monitored immediately afterwards for 60 min. The number of beam breaks was recorded in 5-min bins.

L-DOPA-induced dyskinesia. Mice received unilateral DT injection into the dorsal striatum ipsilateral to the 6-OHDA-injected side. Fifteen days later, they received a single daily injection of L-DOPA (20 mg/kg) and benserazide hydrochloride (10 mg/kg) for 21 days. The abnormal involuntary movements (AIMs) were assessed by two investigators blind of subject genotype for 1 min every 20 min from 20 to 120 min after the last injection on day 21. Axial, limb, and orolingual AIMs were scored using a previously established scale from 0 to 4 for each AIM subtype (Lundblad *et al*, 2004), and the sum of the three scores, defined as dyskinesia score, was determined for each animal (maximal score, 12). Locomotive AIM was expressed as the number of contralateral rotations per minute for each animal.

Open field. The open-field chamber ($50 \times 50\,cm^2$ with a 30 cm-high white plastic wall) was virtually divided into a central field (center, $25 \times 25\,cm^2$) and an outer field (periphery). The open-field test consisted of a 5-min session and was conducted under dim lighting conditions (12 Lux). Individual mice were placed in the center of the field, and the paths of the animals were recorded by a video camera. The distance traveled in the different zones was analyzed by a video-tracking software (Viewpoint Life Sciences, Lyon, France).

Elevated plus maze. The apparatus is elevated 50 cm above the floor and consisted of four arms (6 cm × 37 cm), two enclosed by 18 cm-high white plastic walls and two open. Light intensity was 12 Lux in open arms and 4 Lux in closed arms. Each trial began with the placement of the mouse in the maze center, facing an open arm. The paths of the animals were recorded for 5 min by a video camera. The distance traveled and the numbers of entries in the open and closed arms were quantified by a video-tracking software (Viewpoint Life Sciences). Mice were tested in the levated plus maze 1 day after the open-field test.

Statistical Analysis

Data are presented as mean ± SEM. Statistical analyses (SigmaStat, v3.1) were performed using the unpaired Student's *t*-test. A nonparametric test (test of Mann–Whitney) was used if the normality or equal variance test failed. Two-way repeated-measured ANOVA followed by

Holm–Sidak post tests was used for analyzing time profiles of AIM scores. A significance of $p<0.05$ was required for rejection of the null hypothesis.

RESULTS

Generation of *Slc35d3*$^{DTR\text{-}GFP}$ Transgenic Mice

To ablate striatonigral MSNs, we used the human DTR, the activation of which by DT induces cell apoptosis. We first checked the ability of the fusion DTR-GFP construct to induce cell death *in vitro*. In wild-type cultured hippocampal neurons expressing DTR-GFP fusion, administration of DT triggered apoptosis of GFP-positive cells (Supplementary Figure S1A). To specifically ablate striatonigral MSNs, we chose to drive the expression of the DTR-GFP construct under the control of a highly enriched striatonigral MSNs gene, *Slc35d3* (Heiman *et al*, 2008; Lobo *et al*, 2006), using the BAC-based strategy (Supplementary Figure S1B). Transgenic mice were generated by injecting the recombined BAC into the pronuclei of hybrid C57Bl/6 × CB1 F1 fertilized oocytes, which were then implanted into pseudopregnant females. The five *Slc35d3*$^{DTR\text{-}GFP}$ transgenic founders obtained (hereafter named DTR mice) were outbred with C57Bl/6 mice. One founder did not breed correctly and was discarded from the study. In the four remaining lines, GFP-positive cells were detected in the striatum of DTR$^+$ mice (Supplementary Figure S1C) with a virtually indistinguishable expression pattern. Intrastriatal DTR-GFP protein levels assessed by western blotting were also similar in all the four lines (data not shown). We next determined in which cell type DTR-GFP was expressed. Retrograde fluorescent microbeads were injected into the SNr (Figure 1a), a main target of striatonigral MSNs. The colocalization of GFP-positive soma in the striatum with microbeads confirmed the expression of DTR-GFP by striatonigral MSNs (Figure 1a). The drastic reduction in GFP fluorescence after DT injection into the dorsal striatum of DTR$^+$ mice indicated an efficient ablation of DTR-GFP-positive cells *in vivo* (Figure 1b). The decrease in GFP fluorescence was observed in the rostro-caudal extent of the dorsal striatum while the ventral part (nucleus accumbens) was preserved (Supplementary Figure S2A). Time course analysis showed that the decrease in GFP fluorescence was progressive from day 1 to day 7; over day 7, the ablation was maximal and did not evolve anymore (Supplementary Figure S2B). All the following experiments were performed around 15 days after DT injection after stabilization of the ablation.

Ablation of Striatonigral MSNs by DT Injection

To test the specificity of striatonigral MSNs ablation, we analyzed markers of the different striatal populations using *in situ* hybridization, RT-qPCR, or immunohistochemistry 15 days after unilateral intrastriatal DT injection into the dorsal striatum. None of the markers examined was altered in the DT-injected side *vs* uninjected side in DTR$^-$ mice. DTR$^+$ mice showed strongly reduced *SP* mRNA, a specific marker of striatonigral MSNs, while *Enk* mRNA, a specific marker of striatopallidal MSNs, was unchanged (Figure 1c and d). Among the four lines, line 4 was selected for subsequent experiments, because it showed the highest decrease of *SP* mRNA (-66.3% *vs* uninjected side, $p<0.001$). RT-qPCR analysis confirmed the significant reduction of *SP* (-0.59-fold *vs* uninjected side, $p<0.01$) and also showed a pronounced decrease in the expression of dopamine D_1 receptor (*Drd1a*: -0.76-fold *vs* uninjected side, $p<0.001$), another gene specifically expressed by striatonigral MSNs. In contrast, three genes enriched in striatopallidal MSNs (dopamine D_2 receptor *Drd2*, *Enk* and Adenosine $A2_A$ receptor *Adora2a*) were not affected by DT injection, confirming the specificity of the ablation (Figure 1e). The levels of cAMP-regulated phosphoprotein-32 (DARPP-32), a protein expressed in both populations of MSNs, were also significantly reduced by 39.2% (data not shown).

Knowing that MSNs project to the SNc (Gerfen, 1984), we examined *TH* mRNA levels in the SNc of DT-injected DTR$^+$ mice and found that it was not altered by striatonigral MSNs ablation (data not shown). We then sought to determine the effect of intrastriatal DT on the two main targets of striatonigral and striatopallidal MSNs, the GABAergic neurons of the SNr and GP, respectively. We examined intraneuronal mRNA levels of the GABA synthesis enzyme *GAD67* as an indirect index of GABA neuron activity. *GAD67* mRNA expression was increased in the SNr of DTR$^+$ mice ($+18.2\%$ *vs* uninjected side, $p<0.05$), consistent with overactivity of this structure due to removal of the inhibitory control exerted by striatonigral MSNs (Figure 1f). In contrast, there was no change in *GAD67* mRNA expression in the GP. Altogether, these data demonstrate that the DTR$^+$ transgenic mice are a reliable and effective model to specifically ablate striatonigral *vs* striatopallidal MSNs and that this ablation has a functional impact on BG output.

The striatum contains three categories of GABAergic interneurons with specific cytochemical markers, parvalbumin, calretinin, or neuropeptide Y/NADPH-diaphorase, and one population of cholinergic interneurons expressing choline acetyltransferase (ChAT) (Kawaguchi, 1993). The density of neurons stained for parvalbumin, calretinin, or NADPH-diaphorase was unaffected by DT injection, whereas the density of ChAT-expressing neurons was decreased by 42.7% ($p<0.01$; Figure 2). To exclude down-regulation of ChAT expression, we examined the effect of DT on another protein also specifically expressed by striatal cholinergic interneurons, the type A tyrosine kinase receptor (TrkA) (Holtzman *et al*, 1992). The density of TrkA-positive cells in the DT-injected side of DTR$^+$ mice was decreased to a similar level than ChAT-positive cells (-41.2% *vs* uninjected side, $p<0.01$; Figure 2). In DTR$^-$ mice, DT injection did not affect ChAT-positive cells' density (uninjected side: 44.20 ± 4.11, injected side: 43.01 ± 3.25, $n=4$ DTR$^-$, $p=0.83$), excluding a peculiar sensitivity of this population to DT compared with other striatal populations.

How one can explain the loss of cholinergic interneurons? Two possibilities: (1) DT injection mediates direct ablation of ChAT-positive neurons; and (2) loss of striatonigral MSNs in the dorsal striatum indirectly interferes with the survival of cholinergic interneurons. To distinguish between these two possibilities, we performed a series of control experiments. Using double staining experiments, we

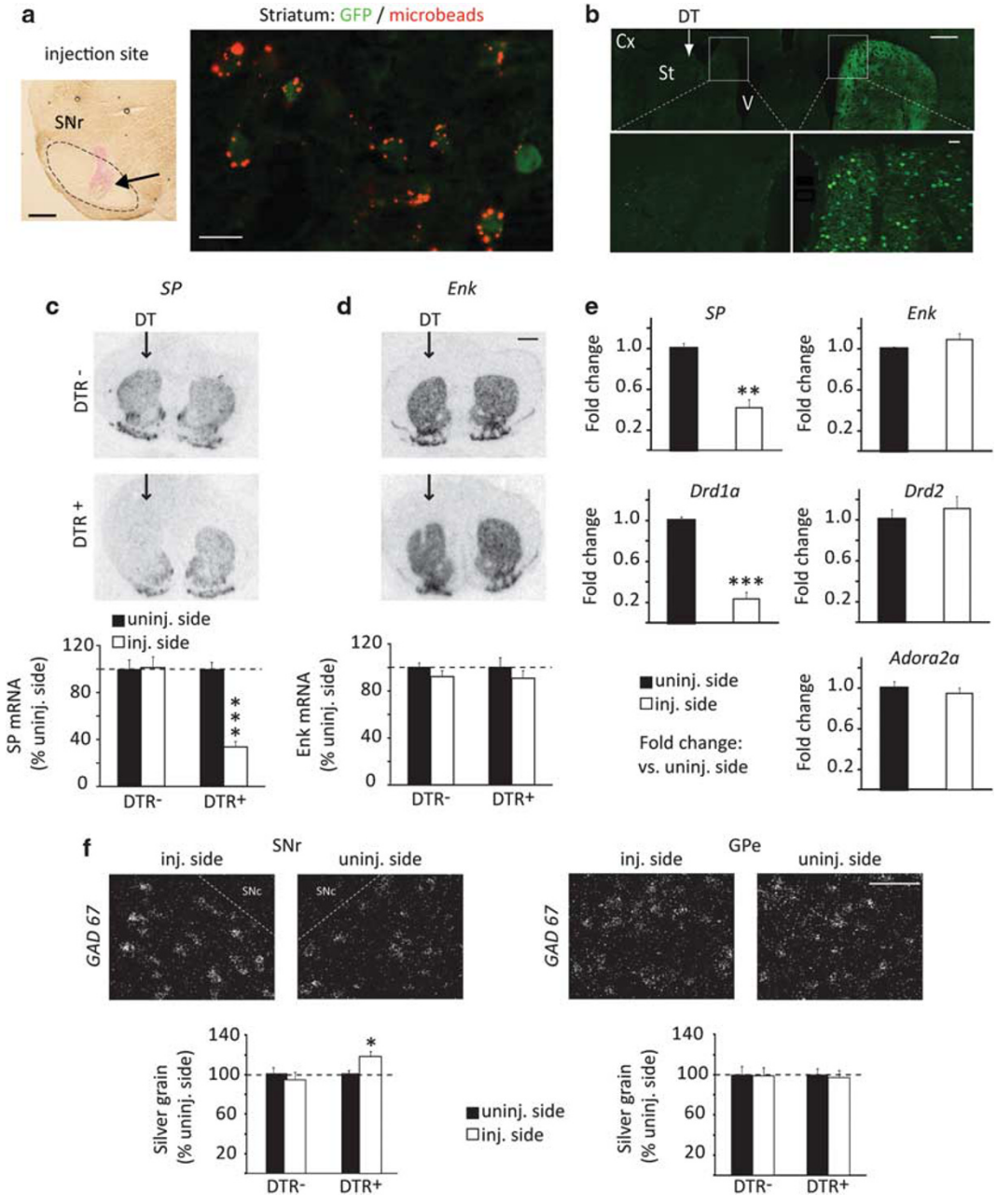

Figure 1 Selective expression of DTR-GFP in striatonigral neurons and impact of DT injection. (a) Left: injection site of fluorescent microbeads indicated by the arrow in the SNr. Scale bar, 200 μm. SNr: substantia nigra pars reticulata. Right: combined immunofluorescence detection of GFP-expressing striatal neurons and retrograde labeling of striatonigral MSNs 7 days after injection of fluorescent microbeads into the SNr of DTR$^+$ mice. The microbeads colocalized with GFP. Scale bar, 10 μm. (b) Striatal GFP immunodetection on a DTR$^+$ coronal brain section 7 days after unilateral DT injection into the striatum showing the loss of GFP expression in the injected side (left) compared with the uninjected side (right). Scale bars, top: 500 μm and bottom: 20 μm. Cx: cortex, St: striatum, V: ventricle. (c, d) Radioactive *in situ* hybridizations and quantification of striatal *SP* (c) and *Enk* (d) mRNA levels 15 days after unilateral DT injections into the striatum of DTR$^-$ ($n=6$) and DTR$^+$ ($n=10$) mice. Arrows indicate the injected side. Scale bar, 1 mm. Data are reported as optical density values and expressed as percentage ± SEM. Student's *t*-test: ***$p<0.001$ *vs* uninjected side. (e) Quantitative RT-qPCR for genes specifically expressed in striatonigral (*SP*, *Drd1a*) or in striatopallidal MSNs (*Enk*, *Drd2*, *Adora2a*). Three DTR$^+$ mice were unilaterally injected with DT into the dorsal striatum, and the total RNA samples from this area were collected in the injected and uninjected side. Results were calculated for each sample relative to the expression of the endogenous reference gene, β-actin, and fold change was determined using the $2^{-\Delta\Delta Ct}$ method. Student's *t*-test: **$p<0.01$, ***$p<0.001$ *vs* uninjected side. (f) Photomicrographs taken under dark-field epi-illumination illustrating intraneuronal *GAD 67* mRNA levels in the SNr and GPe of DTR$^+$ mice, 15 days after DT injections. Scale bar, 100 μm. Quantitative analysis of the number of silver grains per neurons in the SNr (left) ($n=5$ DTR$^-$ and 5 DTR$^+$) and GPe (right) ($n=5$ DTR$^-$ and 6 DTR$^+$). Data are expressed as percentage ± SEM. Student's *t*-test: *$p<0.05$ *vs* uninjected side.

performed a thorough examination of DTR expression in cholinergic interneurons. We found no colocalization between GFP and ChAT proteins in the striatum of DTR$^+$ mice (Figure 3a). Using double *in situ* hybridization, we found no expression overlap between *ChAT* and *DTR*, whereas all *SP*-expressing cells were *DTR* positive

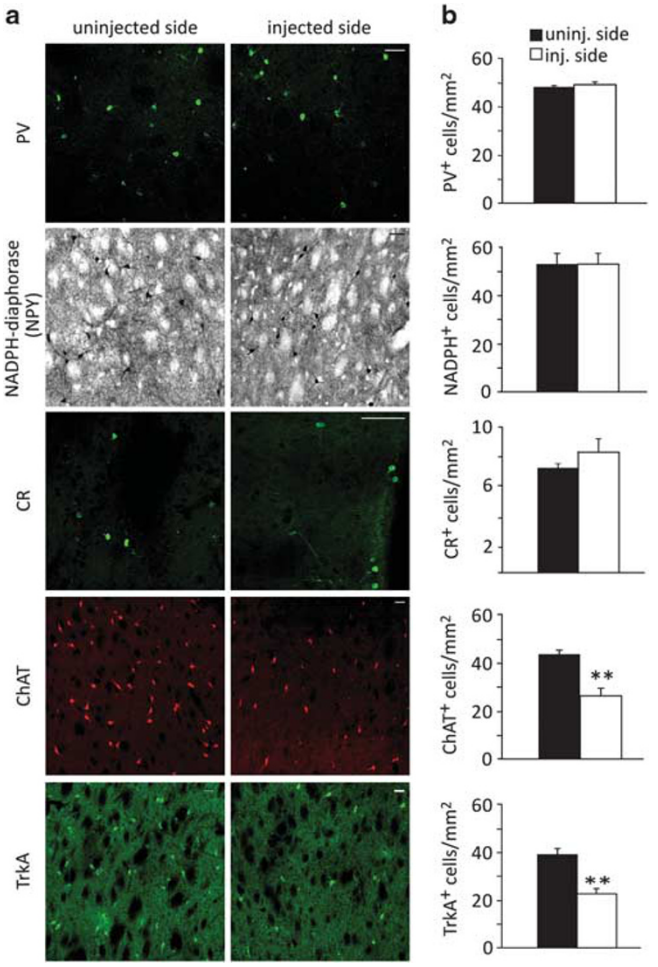

Figure 2 Consequences of striatonigral neuron ablation on striatal interneurons. (a) Coronal sections from DTR$^+$ mice unilaterally injected with DT were stained 15 days after injections for specific markers of GABAergic interneuron subpopulations (parvalbumin, PV; NADPH diaphorase to identify NPY interneurons, calretinin, CR) and for two markers of cholinergic interneurons (choline acetyltransferase, ChAT; type A tyrosine kinase receptor, TrKA). Scale bars, 50 μm. (b) Quantitative analyses illustrate the density of positive cells in the injected and uninjected sides ($n=4$ DTR$^+$). Data are expressed as mean ± SEM. Student's *t*-test: $^{**}p<0.01$ *vs* uninjected side.

(Figure 3b). To further confirm the lack of expression of DTR in cholinergic interneurons, we used single-cell RT-PCR. MSNs and cholinergic interneurons were identified by their distinctive morphological features and firing patterns recorded in cell-attached mode: MSNs have small soma and do not fire action potentials, whereas cholinergic interneurons have large soma and are the only striatal cells in slices that discharge spontaneously. *ChAT* mRNA was never detected in neurons expressing DTR ($n=9$), and *DTR* mRNA was never detected in the neurons expressing ChAT ($n=8$) (Figure 3c). Altogether, these results demonstrate that the loss of cholinergic interneurons is not due to a direct effect of the toxin but is rather an indirect consequence of striatonigral MSNs ablation. This hypothesis is further strengthened by the time course analysis of cell loss we performed from 1 up to 22 days post-DT injection. We found that the loss of ChAT-positive cells was positively correlated to the loss of GFP fluorescence (reflecting MSNs ablation) and that a critical threshold of striatonigral MSNs ablation (>40%) is required to impact cholinergic interneurons' viability (Figure 3d). Finally, as the nucleus accumbens is very similar to the dorsal striatum in terms of cellular composition, we examined the effect of a full ablation of striatonigral MSNs by injecting DT into both regions in the same mouse. Cholinergic interneurons in the dorsal striatum were significantly decreased ($p<0.001$) while those located in the nucleus accumbens were not affected ($p=0.12$), showing that cholinergic interneurons dependence on striatonigral MSNs is territory specific (Figure 3e).

Behavioral Characterization

Behavioral experiments were conducted on G3 mice 15 ± 3 days after intrastriatal DT injection in the dorsal striatum. Injections were made bilaterally except for LID (unilateral injection in the dopamine lesioned side). Animals included in the behavioral analyses were selected *a posteriori* based on marked reduction of *SP* mRNAs determined by *in situ* hybridization in the dorsal striatum ($-63.27\pm2.78\%$, $n=27$ DTR$^+$ mice, $p<0.001$). In addition, we also quantified the level of *SP* mRNAs in the nucleus accumbens in animals used in the open-field and elevated plus maze tests and found no significant change ($-11.10\pm4.91\%$, $n=10$ DTR+ mice, $p=0.07$). Performances of DTR$^+$ mice were compared with their control DTR$^-$ littermates.

Basal and cocaine-induced locomotion is altered in DT-injected DTR$^+$ mice. The dorsal striatum is involved in the regulation of motor activity and motor response to psychostimulants. We therefore examined basal locomotor activity and drug-induced locomotion after cocaine injection, a drug of abuse that increases locomotion by potentiating dopamine signaling. DTR$^+$ mice exhibited significantly reduced basal locomotion during the 60-min test duration compared with DTR$^-$ mice ($p<0.05$) (Figure 4a). When acutely challenged with 15 mg/kg cocaine, both DTR$^-$ and DTR$^+$ mice showed an increased activity compared with their respective saline-injected group (DTR$^-$ cocaine: +134.90% *vs* DTR$^-$ saline, $p<0.001$; DTR$^+$ cocaine: +302.24% *vs* DTR$^+$ saline, $p<0.001$) (Figure 4a). To be unbiased by the hypolocomotion of DTR$^+$ mice, the cocaine-induced locomotor activity was normalized for each genotype to the respective basal activity recorded in saline-injected mice. The locomotor response to cocaine observed in DTR$^+$ mice greatly exceeded the one observed in DTR$^-$ mice (+71.83% *vs* DTR$^-$ mice, $p<0.01$). To further confirm the hypersensitivity of DTR$^+$ mice to cocaine, we tested the effect of a lower dose of cocaine in another two groups of mice. A similar enhancement of the locomotor response to cocaine 5 mg/kg was found in DTR$^+$ mice (+72.90% *vs* DTR$^-$ mice, $p<0.05$; Figure 4b).

L-DOPA induced dyskinesia are strongly reduced in DT-injected DTR$^+$ mice. Dyskinesia is a common complication of L-DOPA pharmacotherapy in PD, affecting a large majority of patients within a few years from treatment onset. LID are associated with biochemical

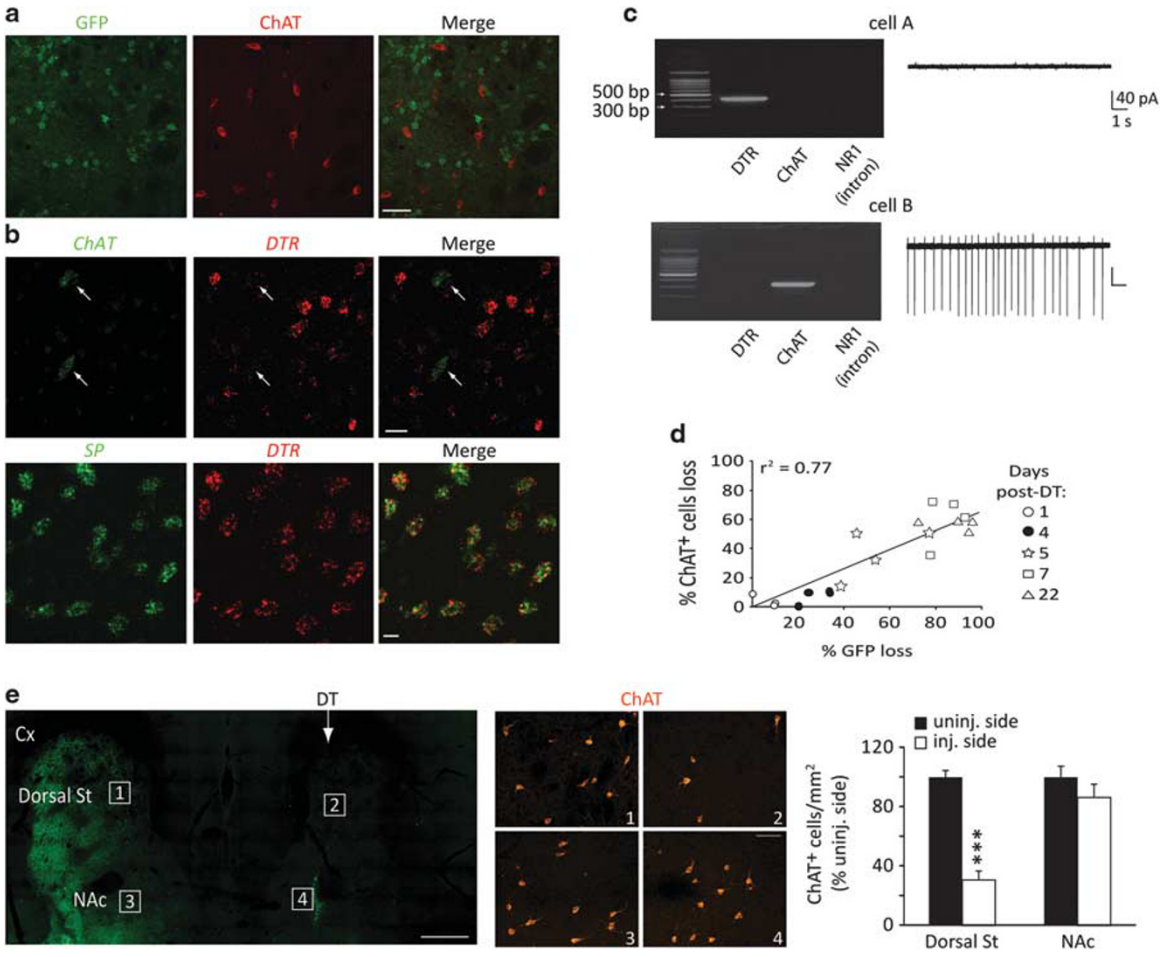

Figure 3 Absence of DTR expression in cholinergic interneurons and characteristics of cholinergic interneuron loss. (a) Double immunofluorescence labeling demonstrated that DTR, revealed by GFP expression (green), does not colocalize with choline acetyltransferase (ChAT) which labels the cholinergic interneurons (red). Scale bar, 50 μm. (b) Dual *in situ* hybridization showing that *DTR* (red) is not expressed in *ChAT*$^+$ cells (green, top, arrows) but colocalized with *SP* (green, bottom). Scale bars, 25 μm (top) and 10 μm (bottom). (c) Agarose gels of the single-cell RT-PCR products from two individual neurons whose electrical activity, recorded in cell-attached mode, is illustrated on the right. *DTR-GFP* mRNA (406 bp) is detected in a silent cell identified as MSN (top) but not in a spontaneous firing cell identified as cholinergic interneuron (bottom) that indeed expresses *ChAT* mRNA (323 bp). Cells are negative for the *NR1* gene intron showing no contamination of the cytoplasm by genomic DNA. (d) The percentage of cholinergic interneurons' (revealed by ChAT staining) and striatonigral MSNs' (revealed by GFP staining) loss, quantified at different time points after unilateral DT injection, is highly correlated. (e) GFP (left) and ChAT (right) immunodetection on a DTR$^+$ coronal brain section 15 days after unilateral DT injection into the dorsal striatum and the nucleus accumbens. Scale bars, left: 500 μm; right: 50 μm. Quantitative analyses illustrate the density of ChAT-positive cells in the dorsal striatum and the nucleus accumbens ($n=6$ DTR$^+$). Cx: cortex, St: striatum, NAc: nucleus accumbens. Data are expressed as percentage ± SEM. Student's *t*-test: ***$p<0.001$ *vs* uninjected side.

alterations of the striatonigral pathway. We therefore examined whether LID expression was affected in DT-injected DTR$^+$ compared with DTR$^-$ mice rendered hemiparkinsonian by unilateral intranigral injection of 6-OHDA (Figure 5a). Strong and equivalent dopaminergic denervation of the striatum ipsilateral to the lesioned side was measured in both DTR$^-$ (-95.5% *vs* uninjected side, $p<0.001$) and DTR$^+$ (-94.9% *vs* uninjected side, $p<0.001$) mice (Figure 5b). After a chronic 21 days of treatment with L-DOPA, DTR$^-$ mice exhibited robust AIMs, which were strongly reduced in DTR$^+$ mice both for dyskinesia (-67.1%, $p<0.001$) and contralateral rotations (-78.4%, $p<0.001$) (Figure 5c). The reduction of AIMs was observed at every time points over the 120-min scoring period following the last L-DOPA injection (repeated-measures ANOVA: genotype effect, $F_{(1,26)}=22.32$, $p<0.001$; time effect, $F_{(5,130)}=50.21$, $p<0.001$; genotype × time interaction, $F_{(5,130)}=18.51$, $p<0.001$; Figure 5d). These results provide direct evidence that striatonigral MSNs ablation can inhibit the expression of LID.

DT-injected DTR$^+$ mice show anxiolytic behavior. The limbic-related connections of the dorsal striatum raise the possibility of its involvement in emotional processing. To test this hypothesis, we assessed our transgenic mice in behavioral paradigms involving an anxiety component: the open field and the elevated plus maze. Mice display anxiety-related behaviors in open spaces; therefore, increased time spent in the central zone of the open field or in the open arms of the elevated plus maze is interpreted

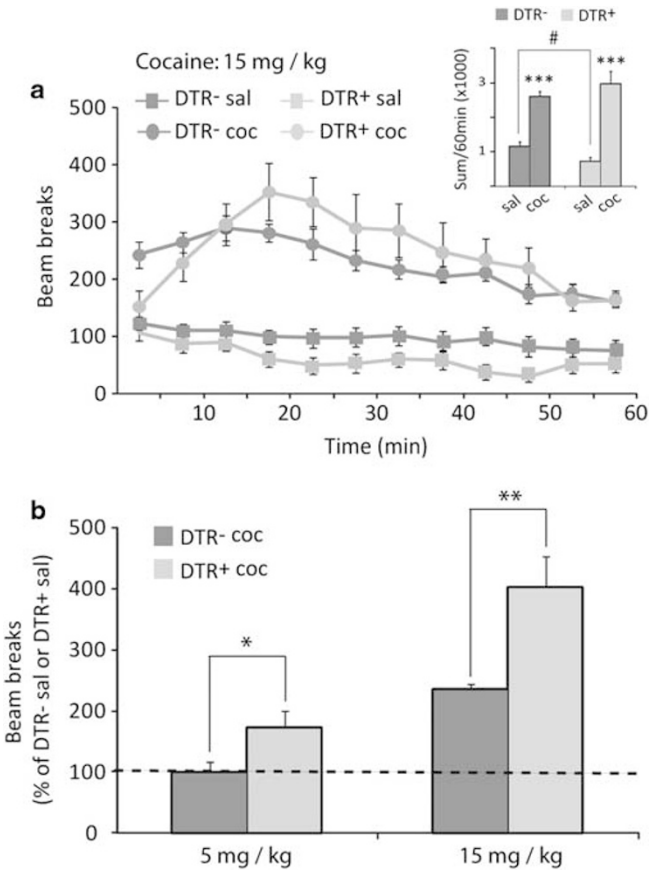

Figure 4 DT injection alters basal and cocaine-induced locomotion. (a) Line graphs illustrate the number of beam breaks in 5-min bins over a 60-min period after saline or cocaine (15 mg/kg) injections for DTR^- ($n=14$ saline and 10 cocaine) and DTR^+ ($n=9$ saline and 6 cocaine) mice. Inset shows the group means ± SEM of total beam breaks for the 60-min test period. Student's *t*-test: $***p<0.001$ *vs* DTR^- sal or DTR^+ sal, $\#p<0.05$ *vs* DTR^- sal. (b) Bar graphs comparing the locomotor response to two different doses of cocaine (5 and 15 mg/kg). Data are the mean number of beam breaks measured during 60 min and are expressed for each genotype as the percentage ± SEM of respective saline-treated mice (5 mg/kg group: DTR^- mice, $n=12$ saline and 12 cocaine and DTR^+ mice, $n=5$ saline and 5 cocaine; 15 mg/kg group: DTR^- mice, $n=14$ saline and 10 cocaine and DTR^+ mice, $n=9$ saline and 6 cocaine). Student's *t*-test: $*p<0.05$, $**p<0.01$ *vs* DTR^- coc.

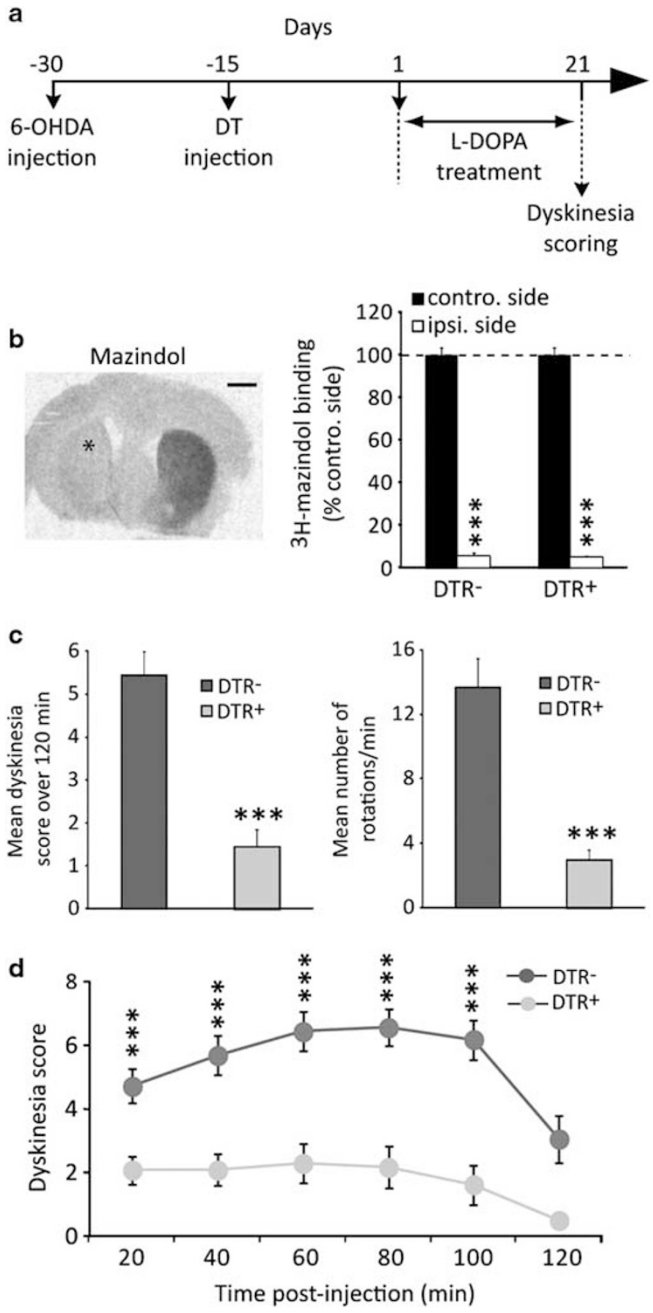

Figure 5 L-DOPA-induced dyskinesia are dramatically reduced after striatonigral neurons ablation. (a) Time course of L-DOPA-induced dyskinesia. (b) Autoradiographic image and quantitative analysis of ^{3}H-mazindol binding showing the extensive loss of dopamine terminals in the striatum ipsilateral to the 6-OHDA injected side (*) ($n=16$ DTR^- and 12 DTR^+). Data are expressed as the percentage ± SEM. Student's *t*-test, $***p<0.001$ *vs* controlateral side. Scale bar, 1 mm. (c) Dyskinesia score (left; sum of the mean scores for axial, orolingual, and forelimb AIMs over 120 min; maximum 12) and locomotive AIM (right; mean number of contralateral rotations per minute over 120 min) after L-DOPA injection on day 21 of chronic treatment ($n=16$ DTR^- and 12 DTR^+). Data are expressed as mean ± SEM. Student's *t*-test, $***p<0.001$ *vs* DTR^- mice. (d) Time profile of axial, limb and orolingual dyskinesia scored every 20 min over a 120-min period after L-DOPA injection at day 21 in DTR^- ($n=16$) and DTR^+ ($n=12$) mice. Data are reported as mean ± SEM. Two-way RM ANOVA: Genotype: $F_{(1,26)}=22.32$, $p<0.001$; time: $F_{(5,130)}=50.21$, $p<0.001$; genotype × time:, $F_{(5,130)}=18.51$, $p<0.001$, Holm–Sidak posttest: $***p<0.001$.

as reduced anxiety. DT-injected DTR^+ mice showed marked increase in the time spent in the central zone of the open field ($p<0.05$) as well as in the time spent ($p<0.001$) and number of entries ($p<0.01$) in the elevated plus maze (Figure 6). These changes reflect reduced anxiety and not a motor impairment as the total distance traveled during the 5-min test period was similar for DTR^- and DTR^+ mice in the open-field (DTR^-: 2958.04 ± 202.53 mm, $n=17$; DTR^+: 2487.03 ± 264.37 mm, $n=10$; NS) and in the EPM (DTR^-: 2094.1 ± 96.7 mm, $n=17$; DTR^+: 2014.8 ± 116.3 mm, $n=10$; NS).

DISCUSSION

In the present study, we achieved inducible striatonigral MSNs' ablation by using cell-type specific expression of DTR and revealed three original results: (i) a region-specific

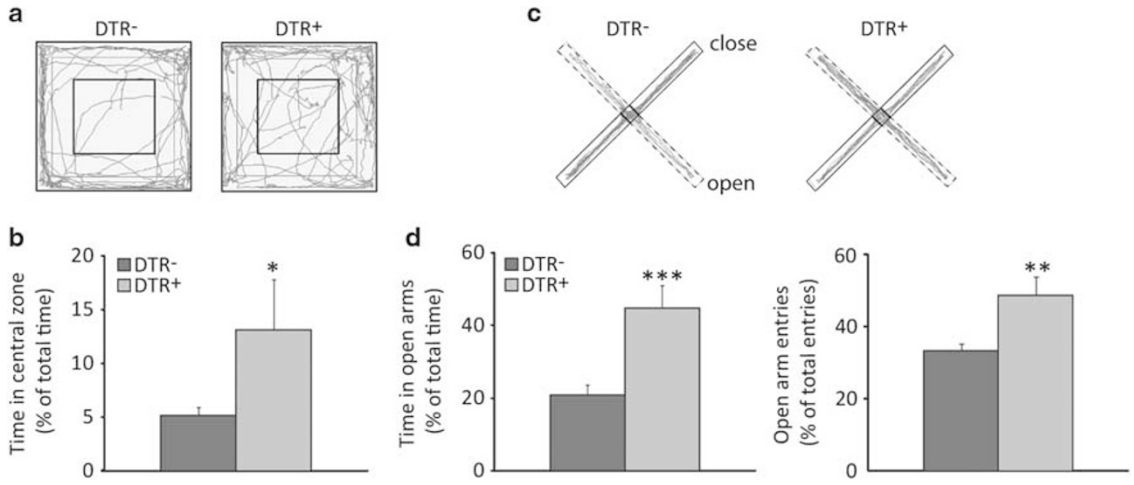

Figure 6 Anxiety is reduced after striatonigral MSNs' ablation. Representative paths (a, c) and quantification showing the time spent in the central zone of the open field (b) as well as the time and the number of entries in the open arms of the elevated plus maze (d) for DTR^- ($n = 17$) and DTR^+ ($n = 10$) mice. Data are expressed as the percentage ± SEM of the total time. Student's *t*-test: $^*p < 0.05$, $^{**}p < 0.01$, $^{***}p < 0.001$ *vs* DTR^- mice.

regulation of cholinergic interneurons homeostasis by striatonigral MSNs, (ii) a causal implication of striatonigral MSNs in L-DOPA-induced dyskinesia, and (iii) the involvement of the dorsal striatum in the regulation of anxiety behavior.

We chose to express DTR under the control of the *Slc35d3* gene promoter based on two studies using FACS (fluorescence-activated cell sorting) and TRAP (translating ribosome affinity purification) that identified *Slc35d3* as the most striatonigral-enriched gene with a restricted expression to the striatum (Heiman *et al*, 2008; Lobo *et al*, 2006). Accordingly, intrastriatal injection of DT into the dorsal striatum triggered not only the elimination of a majority of striatonigral MSNs but also of a portion of cholinergic interneurons. We performed a series of experiments suggesting that the cholinergic loss, which occurred specifically in the dorsal but not in the ventral striatum, is the consequence of striatonigral MSNs' ablation. Another study, in which ablation of striatonigral MSNs is also obtained by DTR activation, reported no change in the number of striatal cholinergic interneurons after DT injection (Durieux *et al*, 2012). In this study, DTR expression in striatonigral MSNs is achieved by crossing iDTR mice (in which DTR expression is under the control of the ubiquitous Rosa26 promoter but is prevented by a loxP-flanked STOP cassette) with D_1-Cre mice. Knowing that transgene expression level is highly dependent on the promoter used to drive its expression, we can assume that DTR level is quite different in the two models. This might also explain the difference in the efficient DT dose between the two studies (0.5 ng/μl *vs* 0.1 ng/μl in Durieux *et al*, 2012); indeed 0.1 ng/μl did not produce significant ablation in our model (not shown). Level of DTR expression might impact the degenerative process, as for instance the kinetics of striatonigral MSNs death and glial reactivity, and differently affect cholinergic interneurons. Reliance of striatal cholinergic survival on non-cell autonomous processes, involving for instance sonic hedgehog signaling from dopaminergic projections, was recently demonstrated in the adult brain (Gonzalez-Reyes *et al*, 2012). In our case, SP released by striatonigral MSNs might be a good candidate to support such pro-survival function as: (i) the presence of numerous SP positive axonal terminals making synaptic contact with dendrites of cholinergic neurons suggests an intimate relationship between these two populations (Bolam *et al*, 1986), (ii) SP biological functions are mediated by the NK1 receptor, which is almost exclusively expressed by cholinergic interneurons in the striatum (Elde *et al*, 1990; Gerfen, 1991), and (iii) NK1 receptor activation triggers pro-survival pathways crucial for the maintenance of some neuronal populations (Chu *et al*, 2011). The differential effects of DT in the striatum and nucleus accumbens open interesting questions and suggest that the cholinergic interneurons have distinct properties in each territory. Further experiments, which are beyond the scope of this study, will be necessary to investigate this region-specific interaction between striatonigal MSNs and cholinergic interneurons.

Our behavioral data showing reduced locomotion in DT-injected DTR^+ mice confirm the BG model of the direct pathway promoting movement and are consistent with recent studies reporting that optogenetic activation or specific ablation of striatonigral MSNs enhances and reduces locomotion, respectively (Durieux *et al*, 2012; Kravitz *et al*, 2010). The increase in *GAD 67* mRNA level in the SNr of DT-injected mice further supports the view that hypolocomotion results from overactive BG outflow subsequent to removal of the inhibitory influence exerted by striatonigral MSNs. In contrast to basal locomotion, our transgenic mice unexpectedly displayed an increase in cocaine-induced activity. Indeed, previous studies reported decreased locomotor response to acute injection of psychostimulants after specifically inhibiting synaptic transmission in striatonigral MSNs (Hikida *et al*, 2010) or ablating these neurons in the striatum (Durieux *et al*, 2012). Differences in the psychostimulant used or the area of the striatum targeted is unlikely to account for such a discrepancy, suggesting that our phenotype might not be the direct consequence of striatonigral damage. Interestingly, an increased sensitivity to acute cocaine has been

reported after elimination of cholinergic cells in the dorsal striatum or the nucleus accumbens (Hikida *et al*, 2001; Sano *et al*, 2003), suggesting that the loss of striatal cholinergic interneurons rather than ablation of striatonigral MSNs might be responsible for the potentiation of cocaine-induced locomotor response.

LID, a major side effect of chronic L-DOPA treatment in PD, are associated with molecular changes occurring specifically in striatonigral MSNs (Santini *et al*, 2009). Our data, showing that striatonigral MSNs ablation prevents the development of LID, provide direct evidence for the causal role of these neurons in LID. This antidyskinetic effect is in agreement with the one obtained after genetic inactivation of DARPP-32 in striatonigral MSNs (Bateup *et al*, 2010). The shift in ERK activation from MSNs to cholinergic interneurons described after long-term exposure to L-DOPA (7 weeks) suggests that the cholinergic interneurons might also be involved in LID expression (Ding *et al*, 2011). Here the beneficial effect of striatonigral MSNs ablation on LID was observed as early as 7 days post-L-DOPA treatment (not shown), a time where ERK activation in cholinergic interneurons is not yet turned on (Ding *et al*, 2011). Thus our results support a primary role of striatonigral MSNs in the development of dyskinesia and also suggest that therapeutic strategies based on manipulation of dopamine-dependent signaling in the striatum should target the striatonigral MSNs for an efficient clinical approach to prevent LID.

Accumulating evidence suggest that the dorsal striatum might also be involved in emotional and motivational processing (Balleine *et al*, 2007). Here we found that DT-injected DTR^+ mice exhibited reduced anxiety in the open-field and elevated plus maze tests. Considering that SP is of relevance in the regulation of emotional states, including anxiety-related behavior (Ebner and Singewald, 2006), and that striatonigral MSNs are the main source of SP in the striatum, our result suggest a role for striatal SP in the regulation of anxiety. Consistent with the anxiolytic effect of striatonigral MSNs ablation, pharmacological blockade or genetic deletion of NK1 receptors produced anxiolytic-like effects (File, 1997; Santarelli *et al*, 2001). As NK1 receptors expressed by cholinergic interneurons are important mediators of SP action in the striatum, the loss of this striatal population in our model is likely to accentuate the anxiolytic effect. SP is widely distributed in the brain and the SP-sensitive areas commonly implicated in the control of anxious states are part of the limbic system (Davis *et al*, 2010). Although the dorsal striatum has limbic connections through the dopamine system (Haber *et al*, 2000), its involvement in anxiety behavior is quite novel and highlights the plurality of neuronal substrates underlying this behavior. Interestingly, dynorphin, another peptide specifically expressed by striatonigral MSNs, has been implicated in anxiety and might thus participate to the reduced anxiety exhibited by the DT-injected transgenic mice (Schwarzer, 2009; Van't Veer and Carlezon, 2013).

Altogether, our data reveal an intimate relationship between striatonigral MSNs and cholinergic interneurons in the dorsal striatum and provide experimental evidence for the implication of these populations not only in dopamine-dependent motor behaviors but also in the control of anxiety, emphasizing the functional overlap between the dorsal striatum and the nucleus accumbens.

FUNDING AND DISCLOSURE

The authors declare no conflict of interest.

ACKNOWLEDGEMENTS

This work was supported by CNRS, Aix-Marseille Université, Fondation de France, Fédération pour la Recherche sur le Cerveau. D.R. was supported by a grant from the Ministry of Education and Research and France Parkinson. We thank A. de Kerchove d'Exaerde for his help in the BAC transgenesis and single-cell RT-PCR experiments, A. Moqrich for helpful discussion and comments on the manuscript, and A. Reynders for her critical comments on the manuscript. We also thank the animal and imaging facilities of the IBDM.

REFERENCES

Albin RL, Young AB, Penney JB (1989). The functional anatomy of basal ganglia disorders. *Trends Neurosci* **12**: 366–375.

Balleine BW, Delgado MR, Hikosaka O (2007). The role of the dorsal striatum in reward and decision-making. *J Neurosci* **27**: 8161–8165.

Bateup HS, Santini E, Shen W, Birnbaum S, Valjent E, Surmeier DJ *et al* (2010). Distinct subclasses of medium spiny neurons differentially regulate striatal motor behaviors. *Proc Natl Acad Sci USA* **107**: 14845–14850.

Bertran-Gonzalez J, Bosch C, Maroteaux M, Matamales M, Herve D, Valjent E *et al* (2008). Opposing patterns of signaling activation in dopamine D1 and D2 receptor-expressing striatal neurons in response to cocaine and haloperidol. *J Neurosci* **28**: 5671–5685.

Beurrier C, Lopez S, Revy D, Selvam C, Goudet C, Lherondel M *et al* (2009). Electrophysiological and behavioral evidence that modulation of metabotropic glutamate receptor 4 with a new agonist reverses experimental parkinsonism. *FASEB J* **23**: 3619–3628.

Bolam JP, Ingham CA, Izzo PN, Levey AI, Rye DB, Smith AD *et al* (1986). Substance P-containing terminals in synaptic contact with cholinergic neurons in the neostriatum and basal forebrain: a double immunocytochemical study in the rat. *Brain Res* **397**: 279–289.

Bolam JP, Wainer BH, Smith AD (1984). Characterization of cholinergic neurons in the rat neostriatum. A combination of choline acetyltransferase immunocytochemistry, Golgi-impregnation and electron microscopy. *Neuroscience* **12**: 711–718.

Cenci MA (2007). Dopamine dysregulation of movement control in L-DOPA-induced dyskinesia. *Trends Neurosci* **30**: 236–243.

Chu JM, Chen LW, Chan YS, Yung KK (2011). Neuroprotective effects of neurokinin receptor one in dopaminergic neurons are mediated through Akt/PKB cell signaling pathway. *Neuropharmacology* **61**: 1389–1398.

Davis M, Walker DL, Miles L, Grillon C (2010). Phasic vs sustained fear in rats and humans: role of the extended amygdala in fear vs anxiety. *Neuropsychopharmacology* **35**: 105–135.

DeLong MR (1990). Primate models of movement disorders of basal ganglia origin. *Trends Neurosci* **13**: 281–285.

Ding Y, Won L, Britt JP, Lim SA, McGehee DS, Kang UJ (2011). Enhanced striatal cholinergic neuronal activity mediates L-DOPA-induced dyskinesia in parkinsonian mice. *Proc Natl Acad Sci USA* **108**: 840–845.

Durieux PF, Bearzatto B, Guiducci S, Buch T, Waisman A, Zoli M *et al* (2009). D2R striatopallidal neurons inhibit both locomotor and drug reward processes. *Nat Neurosci* **12**: 393–395.

Durieux PF, Schiffmann SN, de Kerchove dA (2012). Differential regulation of motor control and response to dopaminergic drugs by D1R and D2R neurons in distinct dorsal striatum subregions. *EMBO J* **31**: 640–653.

Ebner K, Singewald N (2006). The role of substance P in stress and anxiety responses. *Amino Acids* **31**: 251–272.

Elde R, Schalling M, Ceccatelli S, Nakanishi S, Hokfelt T (1990). Localization of neuropeptide receptor mRNA in rat brain: initial observations using probes for neurotensin and substance P receptors. *Neurosci Lett* **120**: 134–138.

Ferguson SM, Eskenazi D, Ishikawa M, Wanat MJ, Phillips PE, Dong Y *et al* (2011). Transient neuronal inhibition reveals opposing roles of indirect and direct pathways in sensitization. *Nat Neurosci* **14**: 22–24.

File SE (1997). Anxiolytic action of a neurokinin1 receptor antagonist in the social interaction test. *Pharmacol Biochem Behav* **58**: 747–752.

Gerfen CR (1984). The neostriatal mosaic: compartmentalization of corticostriatal input and striatonigral output systems. *Nature* **311**: 461–464.

Gerfen CR (1991). Substance P (neurokinin-1) receptor mRNA is selectively expressed in cholinergic neurons in the striatum and basal forebrain. *Brain Res* **556**: 165–170.

Gerfen CR, Engber TM, Mahan LC, Susel Z, Chase TN, Monsma FJ Jr. *et al* (1990). D1 and D2 dopamine receptor-regulated gene expression of striatonigral and striatopallidal neurons. *Science* **250**: 1429–1432.

Gonzalez-Reyes LE, Verbitsky M, Blesa J, Jackson-Lewis V, Paredes D, Tillack K *et al* (2012). Sonic hedgehog maintains cellular and neurochemical homeostasis in the adult nigrostriatal circuit. *Neuron* **75**: 306–319.

Graybiel AM (2000). The basal ganglia. *Curr Biol* **10**: R509–R511.

Haber SN, Fudge JL, McFarland NR (2000). Striatonigrostriatal pathways in primates form an ascending spiral from the shell to the dorsolateral striatum. *J Neurosci* **20**: 2369–2382.

Heiman M, Schaefer A, Gong S, Peterson JD, Day M, Ramsey KE *et al* (2008). A translational profiling approach for the molecular characterization of CNS cell types. *Cell* **135**: 738–748.

Hikida T, Kaneko S, Isobe T, Kitabatake Y, Watanabe D, Pastan I *et al* (2001). Increased sensitivity to cocaine by cholinergic cell ablation in nucleus accumbens. *Proc Natl Acad Sci USA* **98**: 13351–13354.

Hikida T, Kimura K, Wada N, Funabiki K, Nakanishi S (2010). Distinct roles of synaptic transmission in direct and indirect striatal pathways to reward and aversive behavior. *Neuron* **66**: 896–907.

Hikida T, Yawata S, Yamaguchi T, Danjo T, Sasaoka T, Wang Y *et al* (2013). Pathway-specific modulation of nucleus accumbens in reward and aversive behavior via selective transmitter receptors. *Proc Natl Acad Sci USA* **110**: 342–347.

Holtzman DM, Li Y, Parada LF, Kinsman S, Chen CK, Valletta JS *et al* (1992). p140trk mRNA marks NGF-responsive forebrain neurons: evidence that trk gene expression is induced by NGF. *Neuron* **9**: 465–478.

Kawaguchi Y (1993). Physiological, morphological, and histochemical characterization of three classes of interneurons in rat neostriatum. *J Neurosci* **13**: 4908–4923.

Kravitz AV, Freeze BS, Parker PR, Kay K, Thwin MT, Deisseroth K *et al* (2010). Regulation of parkinsonian motor behaviours by optogenetic control of basal ganglia circuitry. *Nature* **466**: 622–626.

Lena C, de Kerchove D'E, Cordero-Erausquin M, le NN, del MA-J, Changeux JP (1999). Diversity and distribution of nicotinic acetylcholine receptors in the locus ceruleus neurons. *Proc Natl Acad Sci USA* **96**: 12126–12131.

Livak KJ, Schmittgen TD (2001). Analysis of relative gene expression data using real-time quantitative PCR and the 2(-Delta Delta C(T)) method. *Methods* **25**: 402–408.

Lobo MK, Covington HE III, Chaudhury D, Friedman AK, Sun H, mez-Werno D *et al* (2010). Cell type-specific loss of BDNF signaling mimics optogenetic control of cocaine reward. *Science* **330**: 385–390.

Lobo MK, Nestler EJ (2011). The striatal balancing act in drug addiction: distinct roles of direct and indirect pathway medium spiny neurons. *Front Neuroanat* **5**: 41.

Lobo MK, Karsten SL, Gray M, Geschwind DH, Yang XW (2006). FACS-array profiling of striatal projection neuron subtypes in juvenile and adult mouse brains. *Nat Neurosci* **9**: 443–452.

Lundblad M, Picconi B, Lindgren H, Cenci MA (2004). A model of L-DOPA-induced dyskinesia in 6-hydroxydopamine lesioned mice: relation to motor and cellular parameters of nigrostriatal function. *Neurobiol Dis* **16**: 110–123.

Nishizawa K, Fukabori R, Okada K, Kai N, Uchigashima M, Watanabe M *et al* (2012). Striatal indirect pathway contributes to selection accuracy of learned motor actions. *J Neurosci* **32**: 13421–13432.

Paxinos G, Franklin KBJ (2001). The Mouse Brain in Stereotaxic Coordinates, 2nd edn. Academic Press: San Diego.

Salin P, Manrique C, Forni C, Kerkerian-Le GL (2002). High-frequency stimulation of the subthalamic nucleus selectively reverses dopamine denervation-induced cellular defects in the output structures of the basal ganglia in the rat. *J Neurosci* **22**: 5137–5148.

Sano H, Yasoshima Y, Matsushita N, Kaneko T, Kohno K, Pastan I *et al* (2003). Conditional ablation of striatal neuronal types containing dopamine D2 receptor disturbs coordination of basal ganglia function. *J Neurosci* **23**: 9078–9088.

Santarelli L, Gobbi G, Debs PC, Sibille ET, Blier P, Hen R *et al* (2001). Genetic and pharmacological disruption of neurokinin 1 receptor function decreases anxiety-related behaviors and increases serotonergic function. *Proc Natl Acad Sci USA* **98**: 1912–1917.

Santini E, Alcacer C, Cacciatore S, Heiman M, Herve D, Greengard P *et al* (2009). L-DOPA activates ERK signaling and phosphorylates histone H3 in the striatonigral medium spiny neurons of hemiparkinsonian mice. *J Neurochem* **108**: 621–633.

Schwarzer C (2009). 30 years of dynorphins–new insights on their functions in neuropsychiatric diseases. *Pharmacol Ther* **123**: 353–370.

Smith Y, Bevan MD, Shink E, Bolam JP (1998). Microcircuitry of the direct and indirect pathways of the basal ganglia. *Neuroscience* **86**: 353–387.

Tai LH, Lee AM, Benavidez N, Bonci A, Wilbrecht L (2012). Transient stimulation of distinct subpopulations of striatal neurons mimics changes in action value. *Nat Neurosci* **15**: 1281–1289.

Van't Veer A, Carlezon WA (2013). Role of kappa-opioid receptors in stress and anxiety-related behavior. *Psychopharmacology (Berl)* **229**: 435–452.

Yawata S, Yamaguchi T, Danjo T, Hikida T, Nakanishi S (2012). Pathway-specific control of reward learning and its flexibility via selective dopamine receptors in the nucleus accumbens. *Proc Natl Acad Sci USA* **109**: 12764–12769.

Supplementary Information accompanies the paper on the Neuropsychopharmacology website (http://www.nature.com/npp)